

# Long room-temperature electron spin lifetimes in highly doped cubic GaN

J. H. Buß,<sup>1</sup> J. Rudolph,<sup>1,a)</sup> T. Schupp,<sup>2</sup> D. J. As,<sup>2</sup> K. Lischka,<sup>2</sup> and D. Hägele<sup>1</sup>

<sup>1</sup>Arbeitsgruppe Spektroskopie der kondensierten Materie, Ruhr-Universität Bochum, Universitätsstraße 150, D-44780 Bochum, Germany

<sup>2</sup>Department of Physics, University of Paderborn, Warburger Str. 100, D-33095 Paderborn, Germany

(Received 22 June 2010; accepted 23 July 2010; published online 9 August 2010)

We report on very long electron spin relaxation times in highly *n*-doped bulk zincblende GaN exceeding 500 ps up to room-temperature. Time-resolved Kerr-rotation measurements show an almost temperature independent spin relaxation time between 80 and 295 K confirming an early prediction of Dyakonov and Perel for a degenerate electron gas. © 2010 American Institute of Physics. [doi:10.1063/1.3478838]

The vision of spin-based semiconductor electronics has stimulated intense research in the field of spintronics.<sup>1</sup> Besides fundamental challenges like spin injection and spin transport, spin relaxation is one of the core problems of spintronics. In contrast to the electron's charge, the spin polarization of an electron ensemble is not a conserved quantity in a semiconductor and decays with time. Most concepts for spintronic devices rely, however, on long spin relaxation times.<sup>2</sup> While spin relaxation can be considerably slowed down in heterostructures, e.g., by employing special crystallographic directions or controlling the electron's orbital motion,<sup>3</sup> long spin relaxation times can hardly be realized in highly doped bulk semiconductors, which are nonetheless required for, e.g., contact layers in devices. Spin relaxation in highly *n*-doped bulk semiconductors is governed by the Dyakonov–Perel spin relaxation mechanism,<sup>4</sup> which is based on an intrinsic conduction-band spin splitting caused by spin-orbit coupling (SOC). The intrinsic spin splitting acts like an effective magnetic field on the electrons' spins, forcing them to precess around the axis of this effective magnetic field  $\mathbf{\Omega}(\mathbf{k})$ . The spin coherence is destroyed by random scattering of the wave vector  $\mathbf{k}$  which leads to a fluctuating effective magnetic field. The spin splitting increases rapidly for occupancy of higher *k*-states, making Dyakonov–Perel relaxation very strong in highly *n*-doped semiconductors. The spin relaxation time  $\tau_s$  decreases like  $\tau_s \propto 1/n^2$  with the doping density *n*, resulting, e.g., in a very short spin relaxation time of only some ps even at cryogenic temperatures for bulk GaAs with  $n=10^{19}$  cm<sup>-3</sup>.<sup>5</sup> The conduction-band spin splitting must be small for increased spin relaxation times. In this context, the wide-gap semiconductor GaN raised considerable interest due to its weak SOC as compared to GaAs. The thermodynamically stable phase of GaN is the wurtzite (WZ) structure which, compared to the zincblende (ZB) structure, gives rise to an additional contribution to the spin splitting. This leads to intrinsic short spin lifetimes.<sup>6</sup> GaN can, however, also be grown in a metastable phase with ZB structure,<sup>7</sup> combining the benefits of the high cubic symmetry and small SOC. Besides the demonstration of long room-temperature exciton spin lifetimes in cubic GaN quantum dots,<sup>8</sup> long electron spin lifetimes were predicted<sup>9,10</sup> for bulk ZB GaN and also first experimental results indicate slow electron spin relaxation in intentionally undoped ZB GaN at low

temperatures.<sup>11</sup> Here, we use time-resolved Kerr-rotation (TRKR) to measure electron spin relaxation times in bulk ZB GaN up to room-temperature. We find very long spin lifetimes despite heavy *n*-type doping.

The ZB GaN (001) sample was grown by plasma assisted molecular beam epitaxy.<sup>12</sup> To avoid carrier escape to the substrate, first a 30 nm thick ZB-AlN (001) barrier was deposited pseudomorphically strained on the 3C–SiC (001) substrate.<sup>13</sup> The top, 570 nm thick ZB-GaN layer was *n*-type doped by Si evaporated from a standard effusion cell. Capacitance-voltage measurements showed a net carrier concentration  $n=(1.0+1.0/-0.5)\times 10^{19}$  cm<sup>-3</sup> at room-temperature. The WZ phase content was found by high resolution x-ray diffraction measurements to be less than the x-ray detection limit of 0.3%. The photoluminescence (PL) spectrum<sup>14</sup> shows the typical behavior of highly *n*-doped bulk semiconductors, with a broad, strongly asymmetric emission band at low temperatures [cf. Fig. 1(a)].<sup>7</sup> The PL spectrum broadens for increasing temperature and becomes more symmetric, with a Gaussian shape at room-temperature [see Fig. 1(a)].<sup>15</sup>

TRKR measurements were performed using femtosecond pump and probe pulses derived from the frequency-doubled output of a mode-locked Ti:Sapphire laser with a

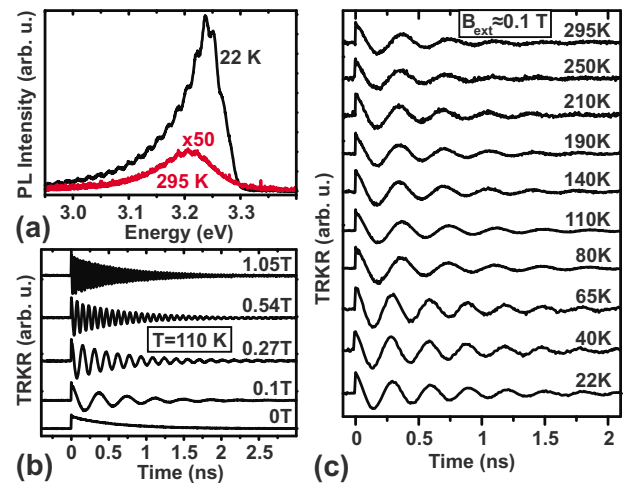


FIG. 1. (Color online) (a) PL spectra at temperatures of 22 and 295 K. The spectrum at 295 K was scaled by a factor of 50. (b) TRKR transients at 110 K for external magnetic fields up to 1 T. (c) TRKR transients for temperatures from  $T=22$  to 295 K in a magnetic field of 0.14 T ( $T\leq 65$  K) and 0.11 T ( $T\geq 80$  K), respectively.

<sup>a)</sup>Electronic mail: joerg.rudolph@ruhr-uni-bochum.de.

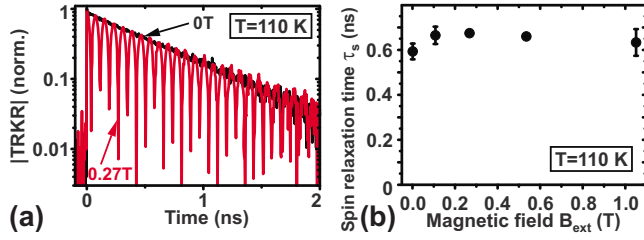


FIG. 2. (Color online) (a) Absolute values of the TRKR transients at a temperature of 110 K without magnetic field and for  $B_{\text{ext}}=0.27$  T on a semi-log scale. (b) Magnetic field dependence of the spin relaxation time  $\tau_s$  at 110 K.

repetition rate of 80 MHz. The polarization of the pump pulse was modulated between left and right circularly polarized, respectively, at 50 kHz by a photo-elastic modulator. The pump beam was focused down to a spot with a diameter of about 60  $\mu\text{m}$  on the sample where a spin-polarized electron ensemble was created. The electron spin dynamics was subsequently monitored via the Kerr rotation of the linearly polarized probe beam that was time delayed by a variable mechanical delay line. The energy of pump and probe beam was varied between 3.29 eV at 22 K and 3.24 eV at 300 K to account for the temperature-induced shift in the band gap. The average pump and probe power was 10 mW and 1 mW, respectively, corresponding to an estimated density of  $n_{\text{exc}}=5 \times 10^{16} \text{ cm}^{-3}$  photoexcited carriers. The sample was kept at temperatures between  $T=22$  and 300 K in a cold-finger cryostat, and an external magnetic field  $B_{\text{ext}}$  was applied in the sample plane.

Figure 1 shows TRKR transients for magnetic fields up to 1 T at a fixed temperature of 110 K [cf. Fig. 1(b)], and for temperatures between 22 and 295 K in a magnetic field of approximately 0.1 T [see Fig. 1(c)]. The oscillations of the TRKR signal in an external magnetic field are due to Larmor precession of the electron spins, while the temporal decay of the TRKR amplitude directly reflects the spin relaxation, which will be discussed in the following. The persistence of the TRKR signal up to times exceeding 2 ns already indicates slow spin relaxation despite the heavy doping of the sample.

In the following, we will first discuss the magnetic field dependence of the spin relaxation. Figure 2(a) compares the absolute values of the TRKR signal without magnetic field and in a field  $B_{\text{ext}}=0.27$  T. Measurements with and without magnetic field are sensitive to the asymmetry of the spin relaxation tensor. Here we find identical spin relaxation times with and without magnetic field and thus, as expected, no anisotropy of the tensor in ZB GaN, in contrast to WZ material, where an intrinsic anisotropy was reported.<sup>16</sup> The spin relaxation time  $\tau_s$  was extracted from the TRKR transients by exponential decay fits<sup>9</sup> of the form  $[A_1 \exp(-t/\tau_c) + A_2] \exp(-t/\tau_s)$  to the zero-field transients, and by a damped cosine fit  $[A_1 \exp(-t/\tau_c) + A_2] \exp(-t/\tau_s) \cos[\omega_L(t-t_0)]$  to the transients for  $B_{\text{ext}} > 0$ , where  $\tau_c$  is a carrier decay time that accounts for a fast initial decay of the optically excited carrier density.<sup>17</sup> Fig. 2(b) demonstrates exemplarily for  $T=110$  K that the spin relaxation time is constant in the whole investigated magnetic field range  $B_{\text{ext}} \leq 1.05$  T.

In the remaining, we will discuss the temperature dependence of the spin relaxation time. The TRKR transients for temperatures between 22 and 295 K look almost identi-

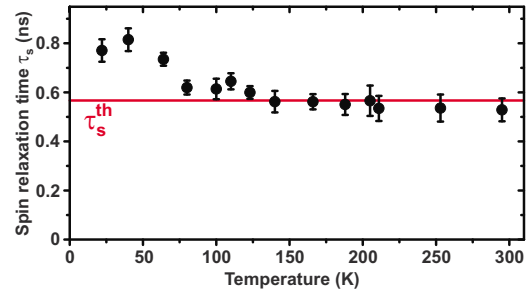


FIG. 3. (Color online) Temperature dependence of the spin relaxation time  $\tau_s$  (full symbols). The line shows the spin relaxation time calculated according to Eq. (3) for  $\tau_p=100$  fs.

cal [Fig. 1(c)]. The spin relaxation time<sup>18</sup>  $\tau_s$  shows correspondingly a very weak temperature dependence (full symbols in Fig. 3), with only a slight increase toward low temperatures. For all temperatures, the spin relaxation time is almost two orders of magnitude longer than the low-temperature value in GaAs at the same doping level,<sup>5</sup> and still reaches  $\tau_s=530$  ps at room-temperature.

The observed very weak temperature dependence of the spin relaxation can be well explained by Dyakonov–Perel theory for the highly degenerate regime as we will show in the following. The SOC-induced conduction-band spin splitting as the basis for Dyakonov–Perel relaxation is in ZB-semiconductors given by the Dresselhaus term<sup>19</sup>  $H_{\text{so}}^D = (\hbar/2)\mathbf{\Omega}(\mathbf{k}) \cdot \boldsymbol{\sigma}$  with the effective magnetic field

$$\mathbf{\Omega}(\mathbf{k}) = \frac{2\gamma_e}{\hbar} \begin{bmatrix} k_x(k_y^2 - k_z^2) \\ k_y(k_z^2 - k_x^2) \\ k_z(k_x^2 - k_y^2) \end{bmatrix}, \quad (1)$$

with the spin splitting constant  $\gamma_e$ . The spin relaxation rate  $\gamma_{ij}$  is in the Dyakonov–Perel formalism obtained from  $\mathbf{\Omega}(\mathbf{k})$  by<sup>20,21</sup>

$$\gamma_{ij}(k) = (\overline{\delta_{ij}\mathbf{\Omega}^2} - \overline{\Omega_i\Omega_j})\tau_p,$$

where  $\tau_p$  is the momentum scattering time and the bar denotes averaging over the directions of  $\mathbf{k}$ .<sup>22</sup> As is expected from the cubic symmetry, the off-diagonal elements of the spin relaxation tensor vanish. The diagonal elements are all equal to

$$\frac{1}{\tau_s(k)} = \frac{32}{105} \frac{\gamma_e^2 k^6}{\hbar^2} \tau_p, \quad (2)$$

where  $k$  corresponds to the Fermi wave vector  $k_F$  for a Fermi-temperature  $T_F=1100$  K given by the doping level  $n=2 \times 10^{19} \text{ cm}^{-3}$ . The spin relaxation time

$$\tau_s = \frac{105\hbar^8}{256\gamma_e^2 E_F^3 m^{*3}} \frac{1}{\tau_p} \quad (3)$$

follows accordingly with the Fermi energy  $E_F = (3\pi^2)^{2/3} \hbar^2 n_D^{2/3} / 2m^*$ . While the first factor in Eq. (3) is approximately temperature-independent, the momentum scattering time  $\tau_p$  will, in general, depend on the temperature. In the degenerate regime, momentum scattering is, however, expected to be dominated by electron-ionized impurity scattering with a temperature-independent scattering time  $\tau_p^i \propto T^0 n_D^0$  in the Brooks–Herring formalism.<sup>23</sup> The spin relaxation time  $\tau_s$  according to Eq. (3) is, therefore, predicted to

be temperature-independent. Assuming a constant momentum scattering time  $\tau_p=100$  fs and using a spin splitting constant<sup>24</sup>  $\gamma_e=0.84$  eV  $\text{\AA}^{-3}$ , a temperature-independent spin relaxation time  $\tau_s^{\text{th}}=567$  ps (solid line in Fig. 3) follows from Eq. (3) for  $n=2 \times 10^{19}$   $\text{cm}^{-3}$  as the upper bound of the doping level.<sup>25</sup> The good agreement with the experiment demonstrates that the spin relaxation is governed by Dyakonov–Perel relaxation (see Fig. 3), giving, to the best of our knowledge, the first systematic experimental demonstration of temperature-independent Dyakonov–Perel relaxation in the highly degenerate regime. The slight increase in the experimental values for  $\tau_s$  toward low temperatures might be caused by the occurrence of localization effects or small changes of the momentum scattering time.

We note that a sample with a higher WZ phase content of 2.5%, resulting from nonoptimal growth conditions, still shows comparably long spin relaxation times, demonstrating the robustness of the long spin lifetimes.

In conclusion, we have investigated the electron spin relaxation in highly  $n$ -doped cubic GaN. The spin relaxation time shows only a weak temperature dependence that is consistent with Dyakonov–Perel relaxation in a highly degenerate regime. Long spin relaxation times  $\tau_s \approx 530$  ps are found even at room temperature, which make cubic GaN a very promising material for future spintronic devices.

We gratefully acknowledge financial support by the German Science Foundation (DFG priority program 1285 ‘Semiconductor Spintronics’ and DFG graduate program GRK 1464 ‘Micro- and Nanostructures in Optoelectronics and Photonics’), J.H.B. was supported by the Ruhr-University Research School funded by Germany’s Excellence Initiative (Grant No. DFG GSC 98/1).

<sup>1</sup>M. I. Dyakonov, *Spin Physics in Semiconductors* (Springer, Berlin, 2008); I. Žutić, J. Fabian, and S. D. Sarma, *Rev. Mod. Phys.* **76**, 323 (2004).

<sup>2</sup>J. Rudolph, D. Hägele, H. M. Gibbs, G. Khitrova, and M. Oestreich, *Appl. Phys. Lett.* **82**, 4516 (2003); M. Oestreich, J. Rudolph, R. Winkler, and D. Hägele, *Superlattices Microstruct.* **37**, 306 (2005).

<sup>3</sup>S. Döhrmann, D. Hägele, J. Rudolph, M. Bichler, D. Schuh, and M. Oestreich, *Phys. Rev. Lett.* **93**, 147405 (2004); O. D. D. Couto, Jr., F. Iikawa, J. Rudolph, R. Hey, and P. V. Santos, *ibid.* **98**, 036603 (2007).

<sup>4</sup>M. I. Dyakonov and V. I. Perel, *Sov. Phys. Solid State* **13**, 3023 (1972).

<sup>5</sup>R. I. Dzhiyev, K. V. Kavokin, V. L. K. M. V. Lazarev, B. Y. Meltser, M. N.

Stepanova, B. P. Zakharchenya, D. Gammon, and D. S. Katzer, *Phys. Rev. B* **66**, 245204 (2002).

<sup>6</sup>J. H. Buß, J. Rudolph, F. Natali, F. Semond, and D. Hägele, *Phys. Rev. B* **81**, 155216 (2010).

<sup>7</sup>D. J. As, in *III-Nitride Semiconductor Materials: Growth*, edited by M. O. Manasreh and I. T. Ferguson (Taylor & Francis, London, 2003), Chap. 9.

<sup>8</sup>D. Lagarde, A. Balocchi, H. Carrère, P. Renucci, T. A. X. Marie, S. Founta, and H. Mariette, *Phys. Rev. B* **77**, 041304 (2008).

<sup>9</sup>S. Krishnamurthy, M. van Schilfgaarde, and N. Newman, *Appl. Phys. Lett.* **83**, 1761 (2003).

<sup>10</sup>Z. G. Yu, S. Krishnamurthy, M. van Schilfgaarde, and N. Newman, *Phys. Rev. B* **71**, 245312 (2005).

<sup>11</sup>A. Tackeuchi, H. Otake, Y. Ogawa, T. Ushiyama, T. Fujita, F. Takano, and H. Akinaga, *Appl. Phys. Lett.* **88**, 162114 (2006).

<sup>12</sup>D. J. As, *Microelectron. J.* **40**, 204 (2009).

<sup>13</sup>T. Schupp, K. Lischka, and D. J. As, *J. Cryst. Growth* **312**, 1500 (2010).

<sup>14</sup>The PL was excited at an energy of 3.52 eV. The oscillatory structures on the PL spectra are due to Fabry–Perot interferences.

<sup>15</sup>J. De-Sheng, Y. Makita, K. Ploog, and H. J. Queisser, *J. Appl. Phys.* **53**, 999 (1982).

<sup>16</sup>J. H. Buß, J. Rudolph, F. Natali, F. Semond, and D. Hägele, *Appl. Phys. Lett.* **95**, 192107 (2009).

<sup>17</sup>A value of  $\tau_c=50$  ps was obtained from time-resolved reflectivity measurements.

<sup>18</sup>The values of  $\tau_s$  shown are averaged over measurements with and without external magnetic field since  $\tau_s$  is independent of the magnetic field and the zero-field measurements are susceptible to drifts during the measurements.

<sup>19</sup>G. Dresselhaus, *Phys. Rev.* **100**, 580 (1955).

<sup>20</sup>D. Hägele, S. Döhrmann, J. Rudolph, and M. Oestreich, *Adv. Solid State Phys.* **45**, 253 (2005).

<sup>21</sup>J. H. Jiang and M. W. Wu, *Phys. Rev. B* **79**, 125206 (2009).

<sup>22</sup>Here we corrected for a wrong sign between the  $\Omega$ -terms, that appears in Eq. (35), page 90 in the often cited Ref. 26.

<sup>23</sup>D. Chattopadhyay and H. J. Queisser, *Rev. Mod. Phys.* **53**, 745 (1981).

<sup>24</sup>With  $m_{cv}=0.092$   $m_e$  from Ref. 10,  $\gamma_e=0.84$  eV  $\text{\AA}^{-3}$  is obtained from the  $k \cdot p$ -formula  $\gamma_e=\alpha\hbar^3/(2\sqrt{2}m^{*3}E_g)$  with the dimensionless constant (Ref. 26)  $\alpha=(4/3)(m^*/m_{cv})\eta[1-(\eta/3)]^{-1/2}$  and  $\eta=\Delta_{so}/(E_g+\Delta_{so})$ , using  $E_g=3.302$  eV (Ref. 27),  $\Delta_{so}=0.017$  eV (Ref. 27), and  $m^*=0.13$   $m_e$  (Ref. 28).

<sup>25</sup>Similarly good agreement is also obtained using the value  $\gamma_e=0.55$  eV  $\text{\AA}^{-3}$  predicted by Fu and Wu (Ref. 29), giving  $\tau_s^{\text{th}}=615$  ps for a reasonable momentum scattering time  $\tau_p=250$  fs.

<sup>26</sup>*Optical Orientation*, edited by F. Meier and B. P. Zakharchenya (North-Holland, Amsterdam, 1984).

<sup>27</sup>G. Ramírez-Flores, H. Navarro-Contreras, A. Lastras-Martínez, R. C. Powell, and J. E. Greene, *Phys. Rev. B* **50**, 8433 (1994).

<sup>28</sup>V. Bougrov, M. Levinshtein, S. Rumyantsev, and A. Zubrilov, in *Properties of Advanced Semiconductor Materials*, edited by M. E. Levinshtein, S. L. Rumyantsev, and M. S. Shur (Wiley, New York, 2001), Chap. 1.

<sup>29</sup>J. Y. Fu and M. W. Wu, *J. Appl. Phys.* **104**, 093712 (2008).